Remote sensing-based research on haze pollution over eastern China

Qin Kai（秦凯）, 中国矿业大学
Bai Yang（白杨）, 中国矿业大学/河南大学
Rao lanlan (饶兰兰), 中国矿业大学/ DLR
Wong Mansing（黄文声）, 香港理工大学
Xu Jian（许健）, DLR
Wu Lixin（吴立新）, 中南大学

Air Quality Monitoring Site of CUMT

代安全上网导航 × XuZhou-CUMT - AERONET ×

GODDARD SPACE FLIGHT CENTER

+ Visit NASA.gov

one long-term site of AERONET since 2013

+ AEROSOL OPTICAL DEPTH | + AEROSOL INVERSIONS | + SOLAR FLUX | + OCEAN COLOR | + MARITIME AEROSOL

Web Site Feature — AERONET Data Synergy Tool - Access Earth Science data sets for AERONET sites

+Home

Home

- + AEROSOL/FLUX NETWORKS
- + CAMPAIGNS
- + COLLABORATORS
- + DATA
- + LOGISTICS
- + NASA PROJECTS
- + OPERATIONS
- + PUBLICATIONS
- - SITE INFORMATION
- + STAFF
- + SYSTEM DESCRIPTION

AERONET DATA ACCESS

AERONET Site Information Database

XuZhou-CUMT (XuZhou, PR China)

Site Index

Image 1

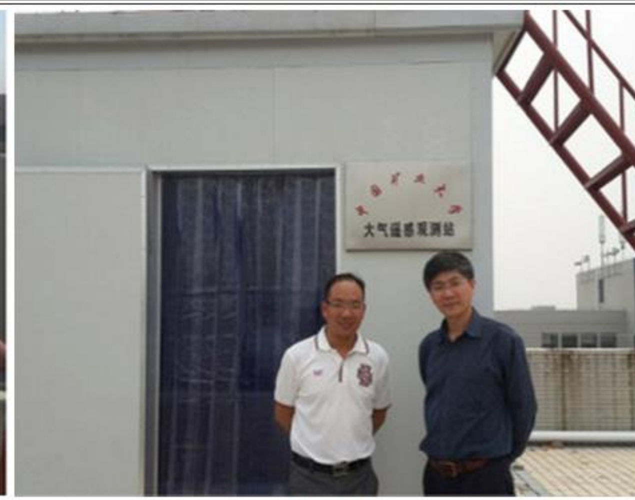

Image 2

Image 1 - The sunphotometer in the roof of School of Environmental Science and Spatial Informatics, China University of Mining and Technology.

Image 2 - The site manager (left) and PI (right).

Site Coodinates and Elevation:	• Latitude: 34.21667° North • Longitude: 117.14167° East • Elevation: 59.7 Meters

Part 1

Investigating haze aerosol optical properties

“石家庄气溶胶时空特征星地协同观测项目”

1、领导小组：

组长：高献计，河北省地理信息局 局长

成员：吕竹青，河北省环境保护厅 副厅长

连志鸾，石家庄市气象局 副局长

2、研究组：

组 长：吴立新教授；

副组长：秦 凯 黄文声

成 员：袁丽梅 王润峰 裴广军 刘 伟 尹志永 陈 刚 周 阳 田时雨 郑 硕 白 杨 吕 鑫 胡明玉 石铁伟 储建松；吴启威 张朝阳

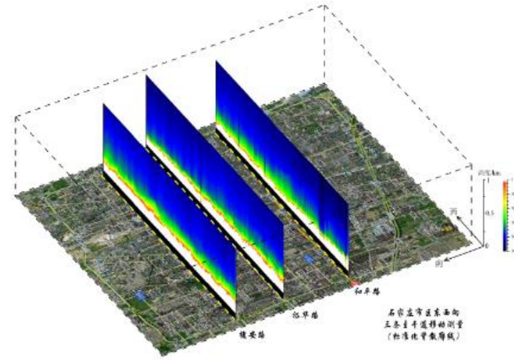

如图4.20所示的NRB数据显示，三条东西向主干道的污染物颗粒垂直空间分布情况基本一致，**市区污染物气溶胶颗粒均在近地面高度聚集。**

图4.20 石家庄市内东西向干路MPL移动观测(NRB)

如图4.21所示DR数据显示，北部的和平路近地面污染物颗粒规则度明显高于南部的裕华路与槐安路，说明**市区南北污染物气溶胶颗粒物来源可能差异。**

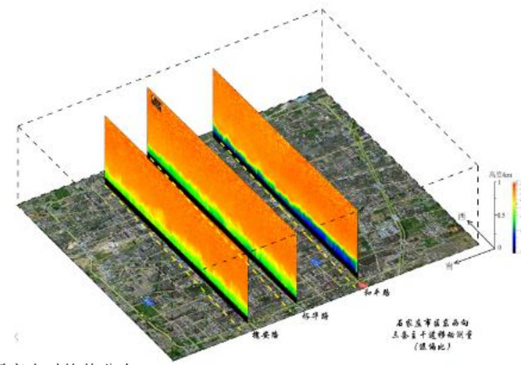

L移动观测(DR)

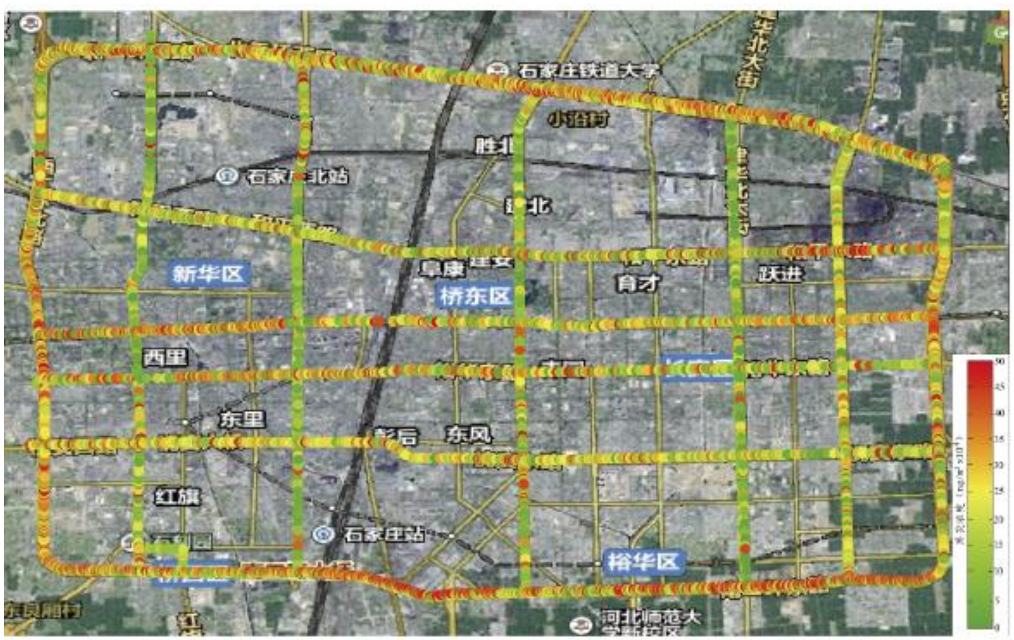

气溶胶光学厚度小时均值分布

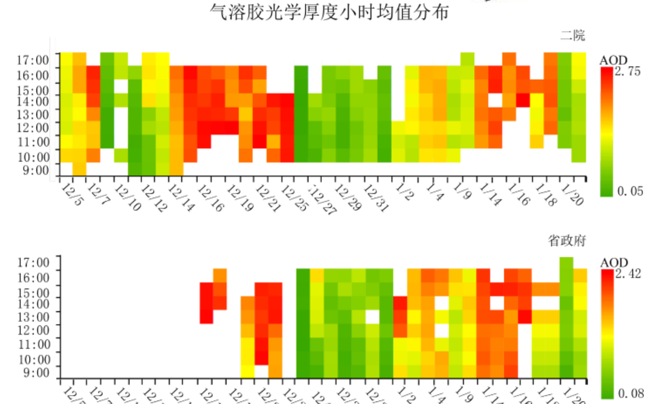

Sites and Measurements

A single channel **aethalometer** (model: AE-16, Magee Scientific) is used to measure black carbon (BC).

The attenuation of light at 880 nm wavelength is converted to the BC mass concentration using wavelength dependent calibration factors.

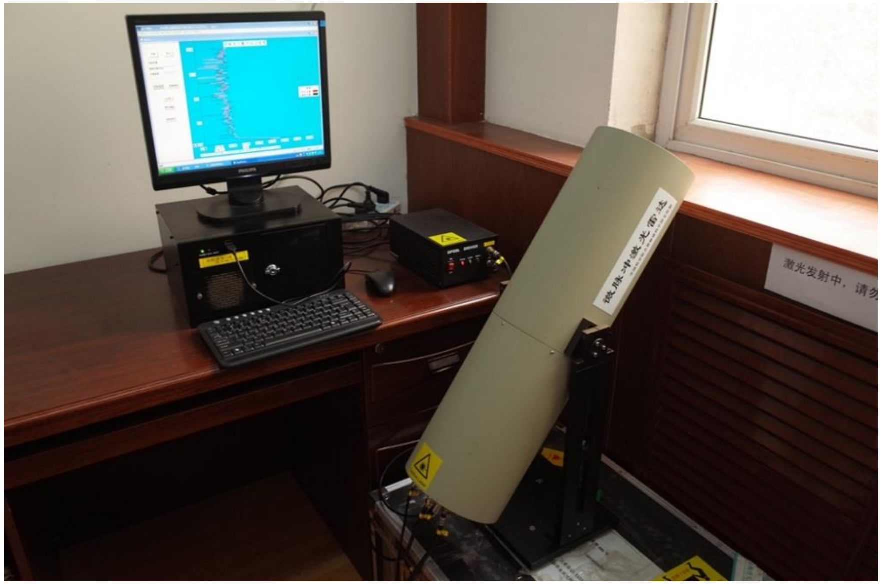

A **micro pulse lidar (MPL)** is used to obtain vertical aerosol distribution.

Aerosol extinction profiles are derived by solving lidar equation using a Fernald algorithm assuming a constant Lidar Ratio (the ratio of the volume backscattering coefficient to the volume extinction coefficient).

Sites and Measurements

省政府站点：

AQI日均值

- 优：0~50
- 良：51~100
- 轻度污染：101~150
- 中度污染：151~200
- 重度污染：201~300
- 严重污染：>300

1	2	3	4	5	6	7	8	…	…	…	…	38	39
12月16日	12月17日	12月18日	12月19日	12月20日	12月21日	12月22日	12月23日	…	…	…	…	1月22日	1月23日

Results and Analysis

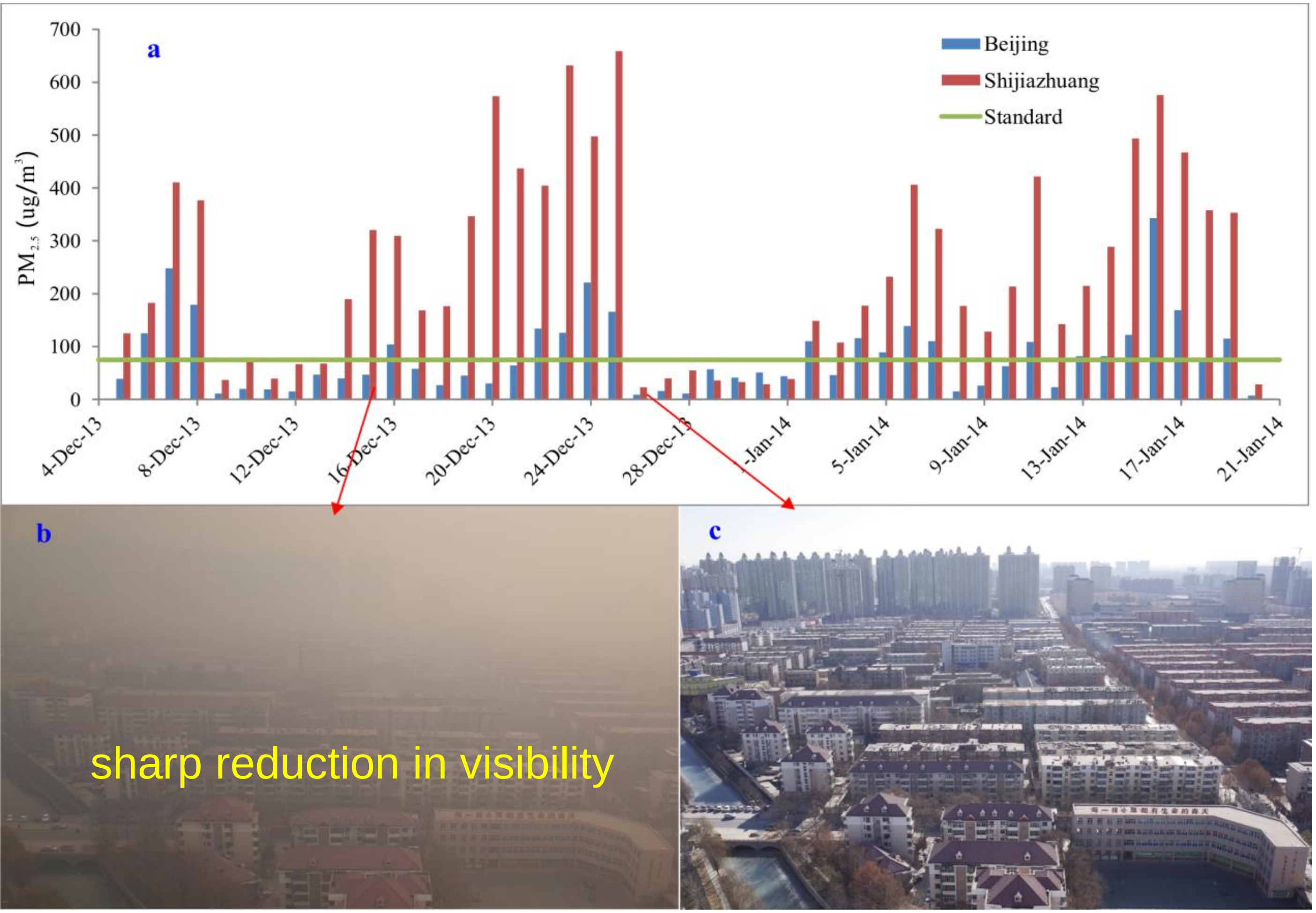

More than 70% and about 45% of the total days were polluted ($PM_{2.5}$>75 μg/m^3) in Shijiazhuang and in Beijing, respectively

More frequent hazes over Shijiazhuang than Beijing

Daily mean value of $PM_{2.5}$ over Shijiazhuang and Beijing in 2013-2014 winter

Results and Analysis

- **Total and fine-mode** (anthropogenic aerosol) AODs show dramatic daily variations.
- **Coarse-mode AOD** (natural aerosol) is generally small and nearly constant.

Daily values of total, fine-mode, and coarse-mode AOD_{500nm} over Shijiazhuang and Beijiing.

Results and Analysis

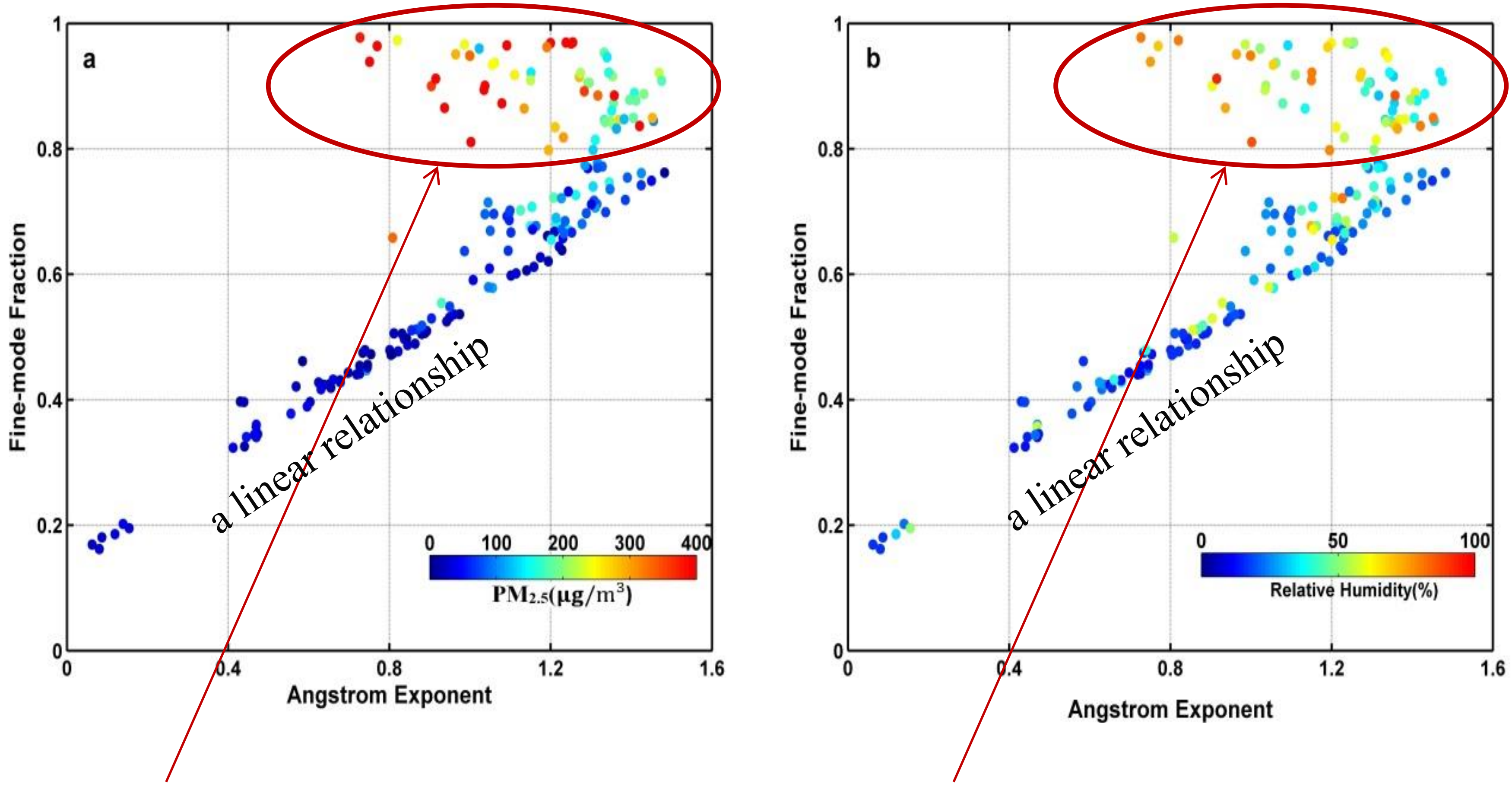

During heavy hazes with higher relative humidity, FMF values are larger than 0.80, the angstrom exponent displays more dispersiveness. This could be attributed to **fine-mode particles augment from hygroscopic growth in the presence of water.**

Results and Analysis

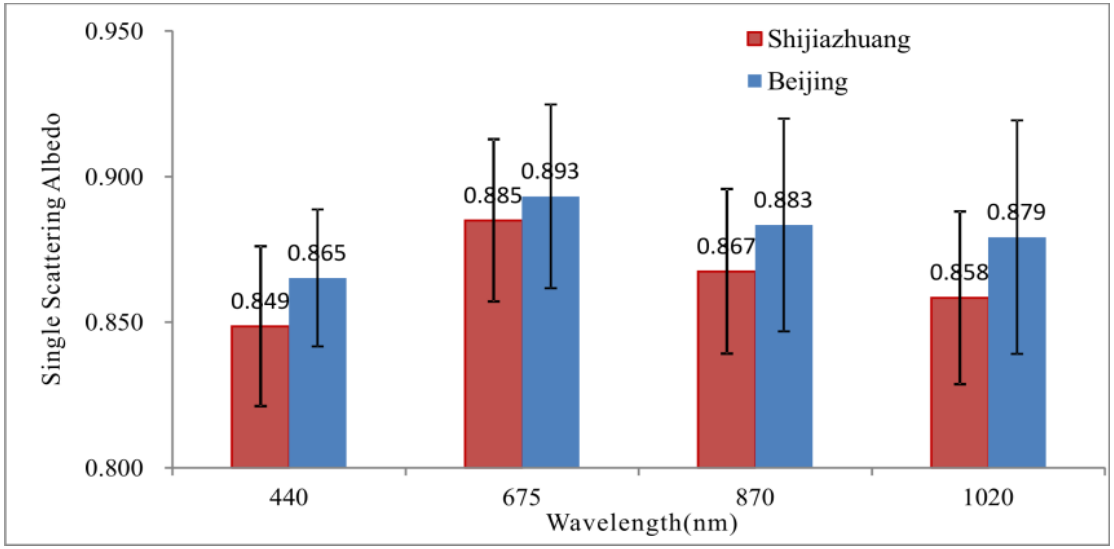

- The presence of spectrally-dependent absorbing aerosols.
- Smaller SSA over Shijiazhuang indicates more absorbing particles (black carbon and brown carbon).

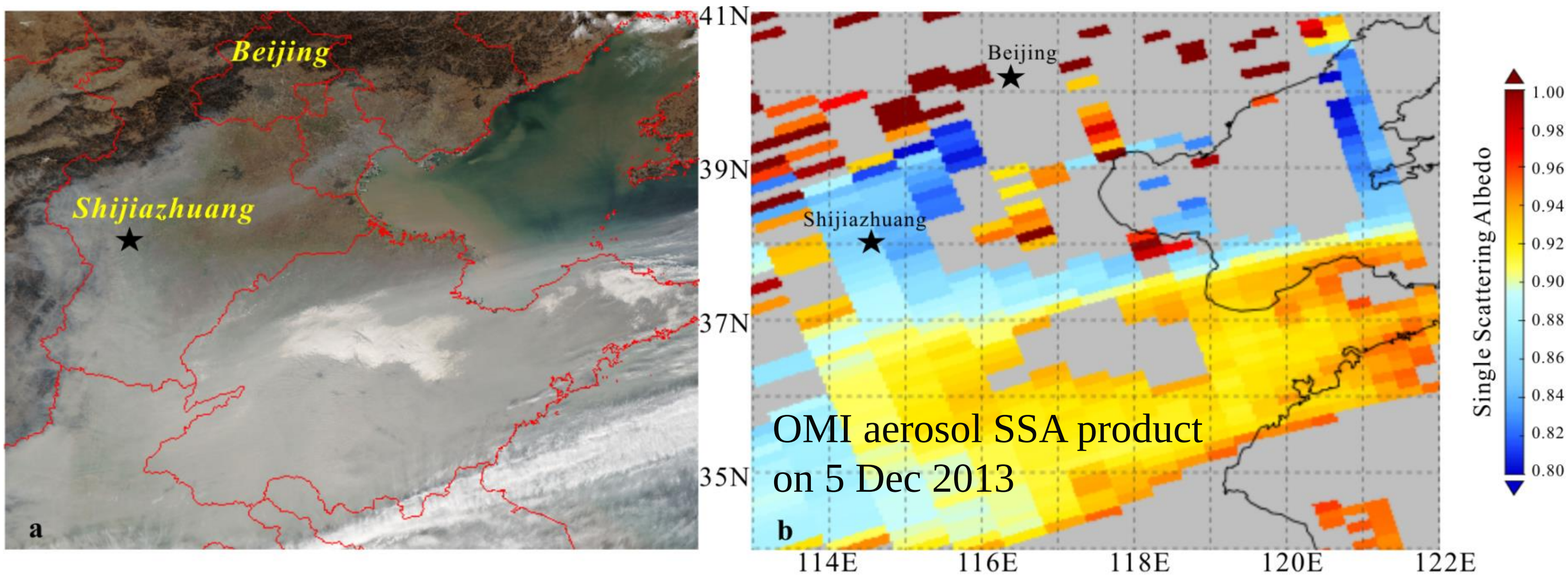

Results and Analysis

High black carbon aerosol during hazes over Shijiazhuang

Table 1 Daily concentrations of BC (μg/m^3), $PM_{2.5}$ (μg/m^3) and their ratios during pollution days

Date	BC	$PM_{2.5}$	BC/ $PM_{2.5}$(%)
Dec.16	40.83	309.67	13.18
Dec.17	19.10	168.63	11.33
Dec.18	21.67	176.57	12.27
Dec.19	42.82	346.39	12.36
Dec.20	68.40	573.67	11.92
Dec.21	44.05	437.04	10.08
Dec.22	55.16	404.38	13.64
Dec.23	74.77	632.04	11.83
Dec.24	69.84	497.91	14.03
Dec.25	69.01	658.92	10.47
Means	50.56	420.52	12.11
Std. deviations	20.16	173.94	1.28

Much larger than 6.60% in Nanjing, 8.33% in Shanghai, and those in other 14 cites in China (Cao et al., 2007).

Results and Analysis

Low boundary layer heights during hazes over Shijiazhuang

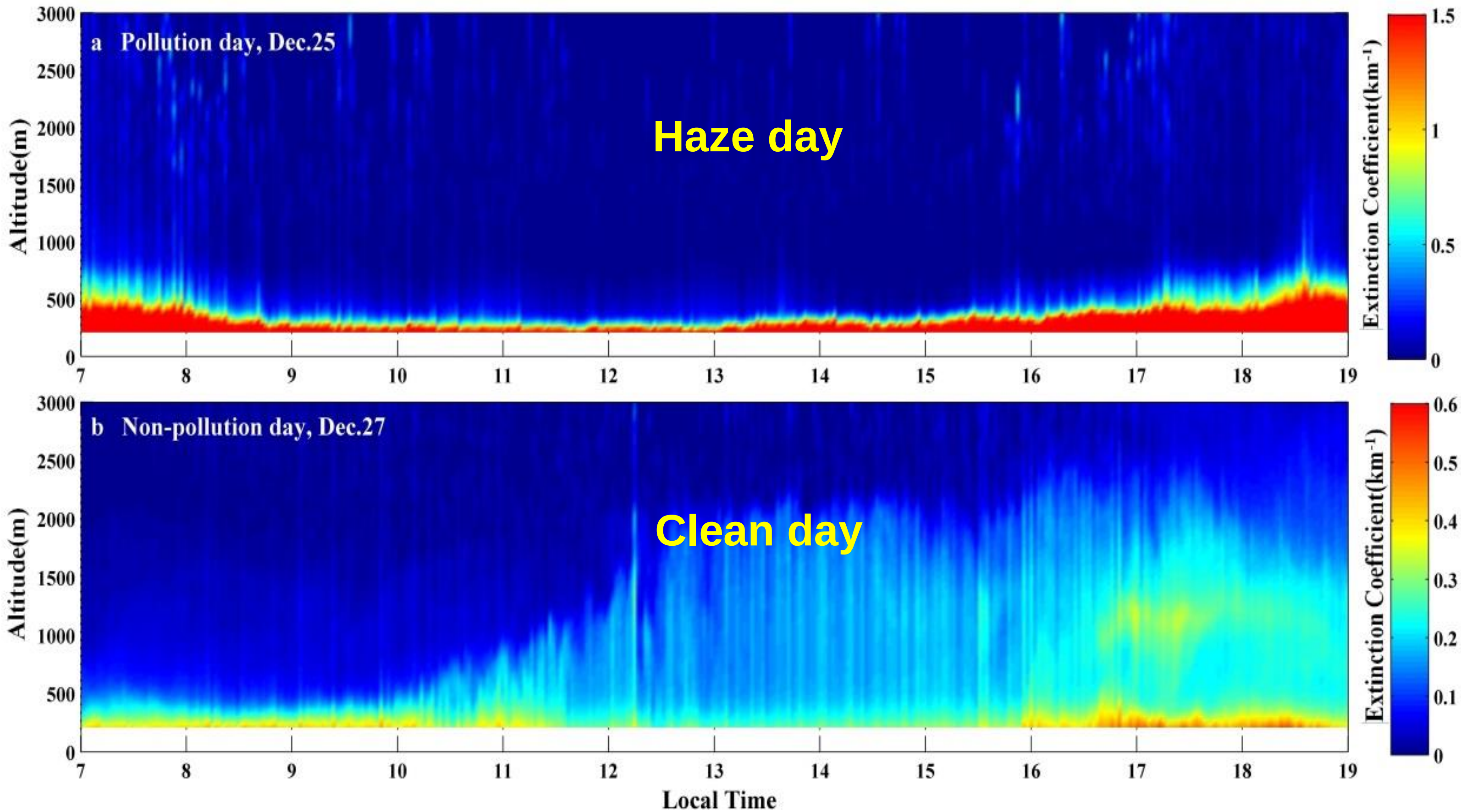

Under fair-weather conditions, the boundary layer is fully developed and actively mixed in the afternoon.

Results and Analysis

Daily max boundary layer height is defined as the averaged afternoon values

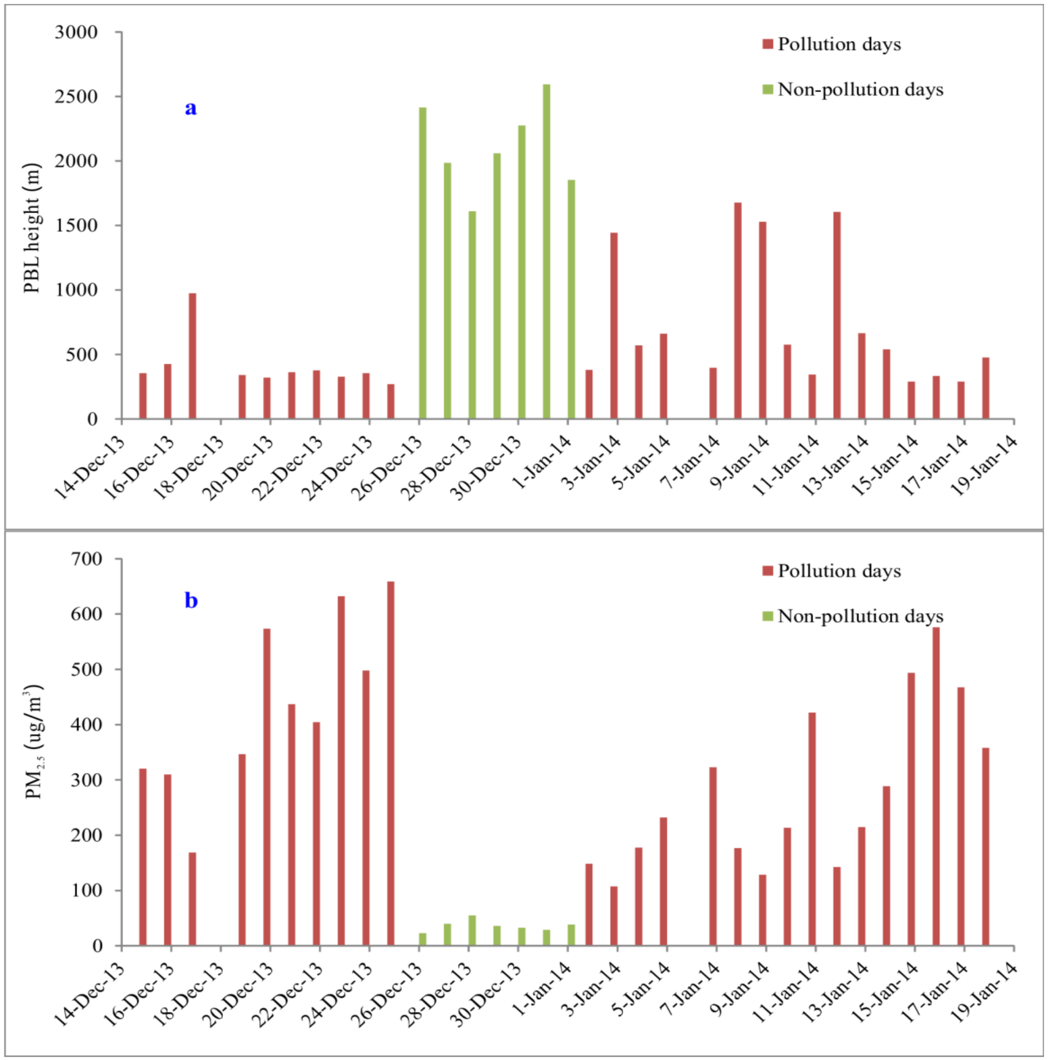

Negative correlation between the daily max boundary layer height and the daily means of $PM_{2.5}$

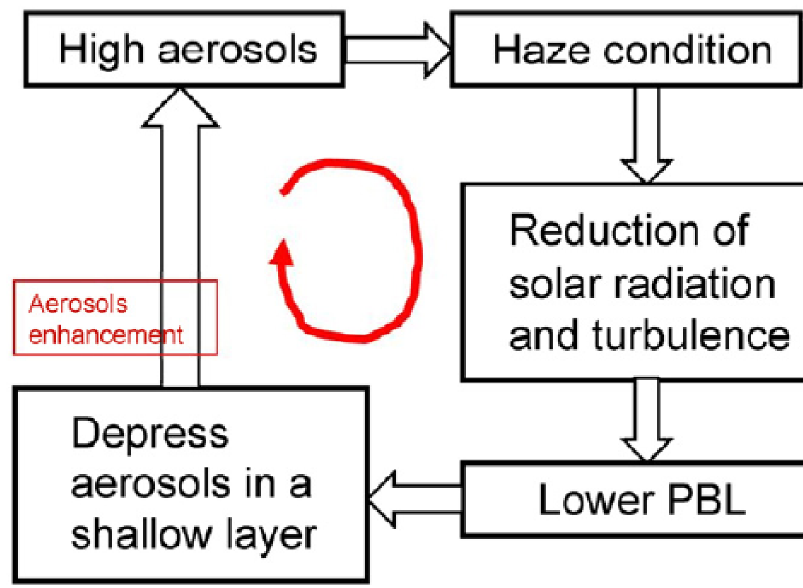

Aerosol-BL feedback loop

Results and Analysis

High BC and low boundary layer height during hazes

The radiative forcing analysis (Ding et al. 2016) suggests that BC plays a key role in heating the atmosphere and cooling the surface, further enhance the stability of the boundary layer.

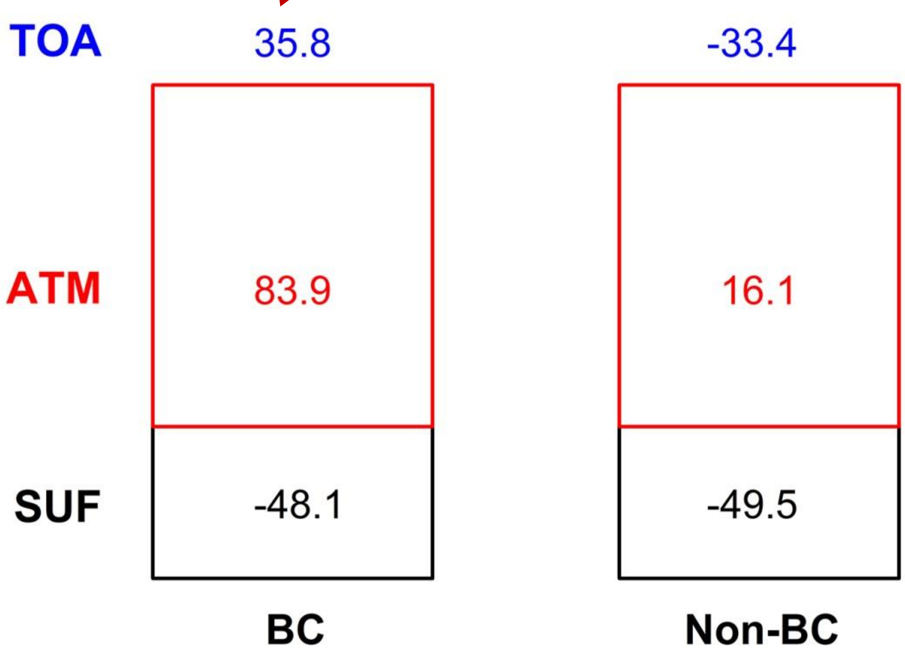

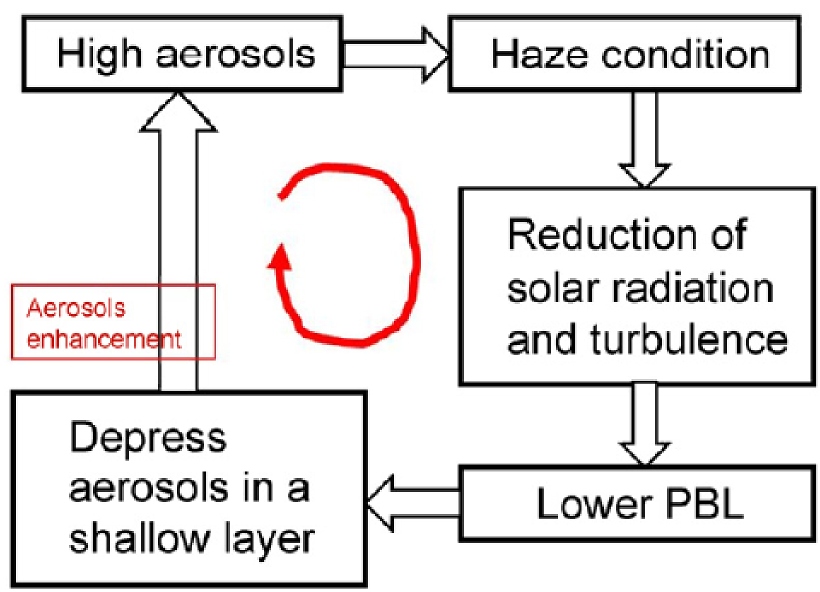

Aerosol-BL feedback loop

Part 2

Detecting aloft haze transport

Motivation

Gravity-Current Driven Transport of Haze from North China Plain to Northeast China in Winter 2010

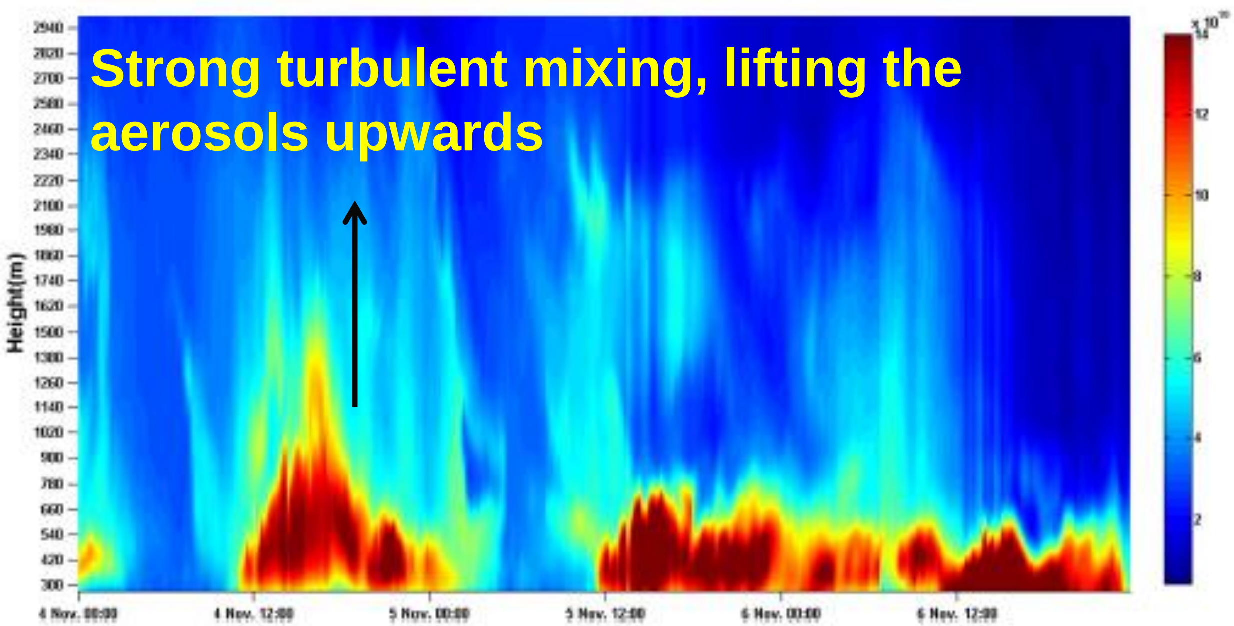

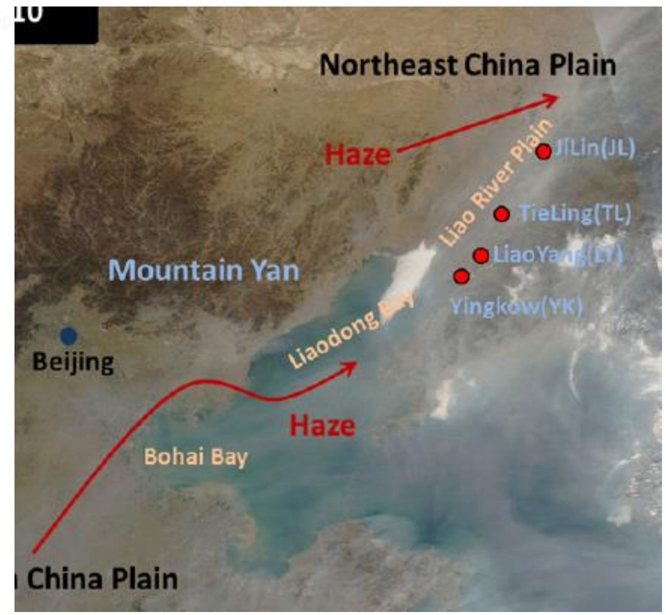

Yang, T., Wang, X., Wang, Z., Sun, Y., Zhang, W., Zhang, B., & Du, Y. (2012). Gravity-current driven transport of haze from North China Plain to Northeast China in winter 2010-Part I: observations. Sola, 8(0), 13-16.

A typical winter haze in China in January 2015

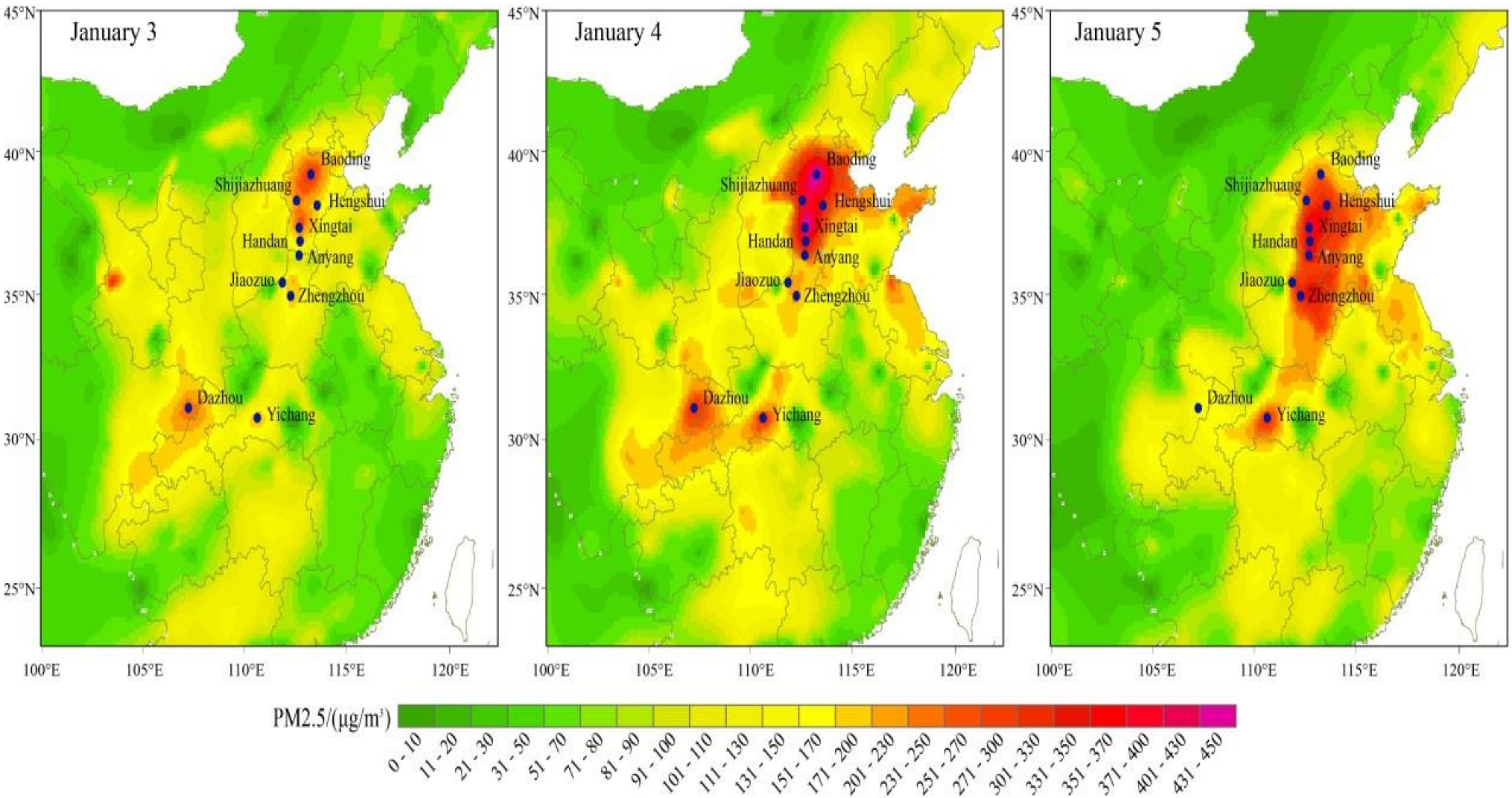

Spatial interpolation of daily $PM_{2.5}$ of 367 cities in central and eastern China

Two-layer structures can be seen from the total attenuated backscatter coefficient images

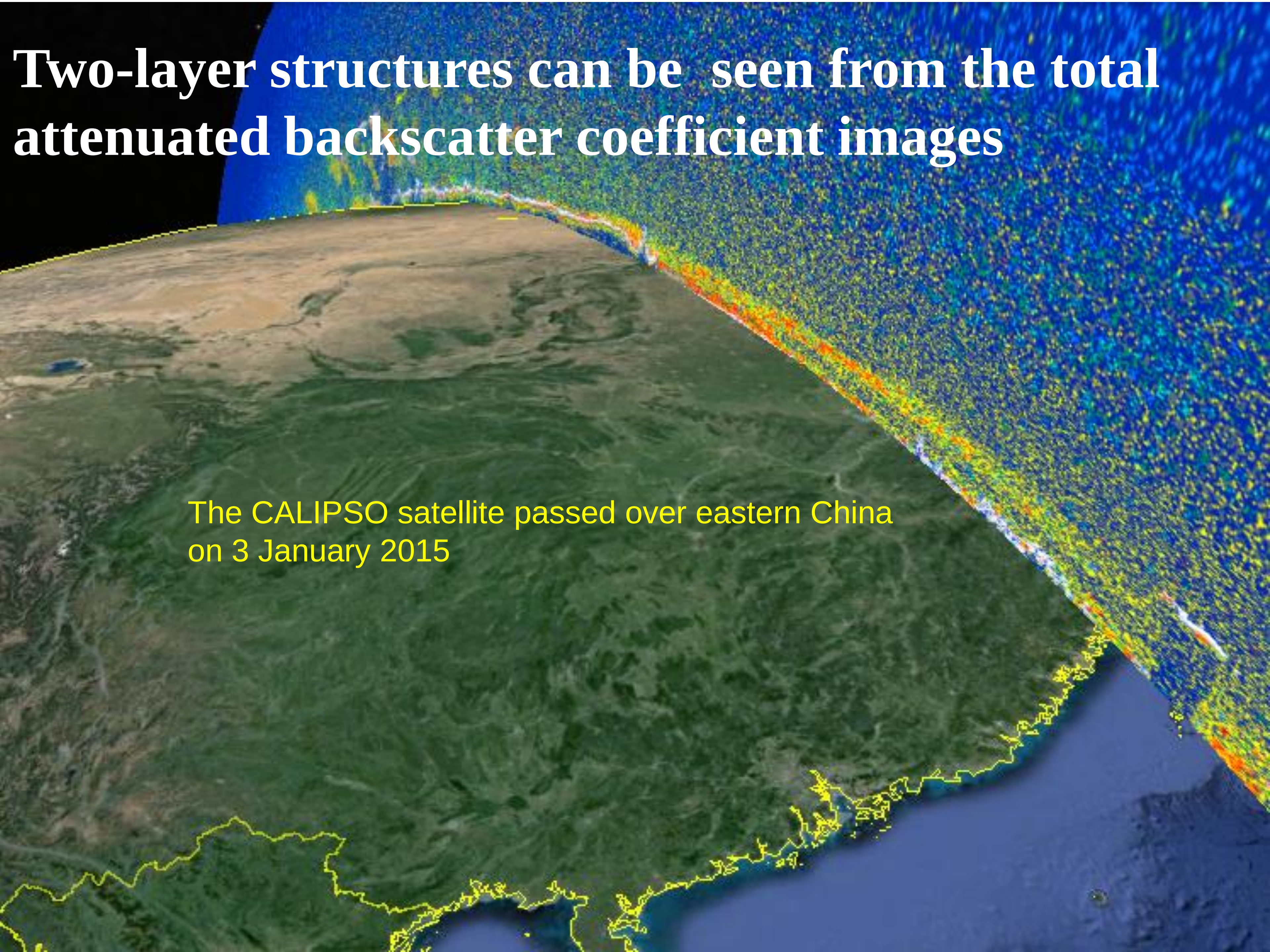

Besides the local pollution layers near the ground, there were high altitude pollutant belts at 2–4 km, classified as smoke

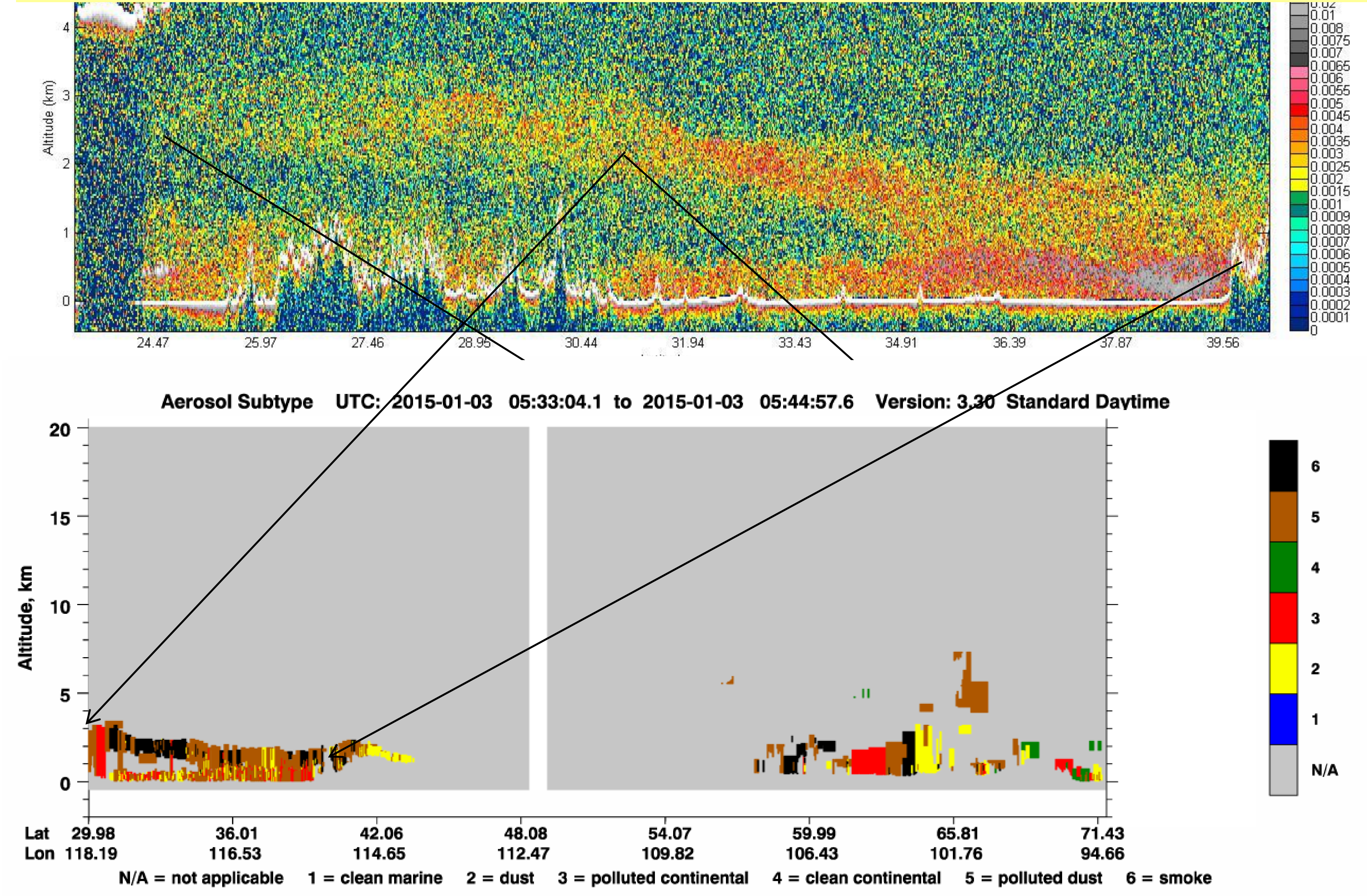

Similar episodes of external aerosol passing through and into the area were seen by ground LIDAR in three cities in eastern China

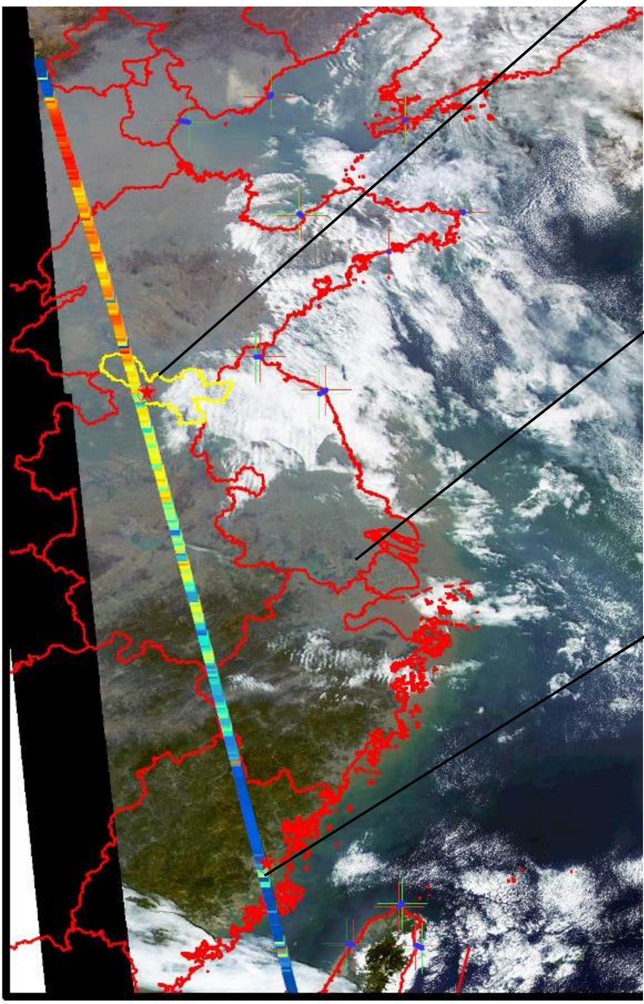

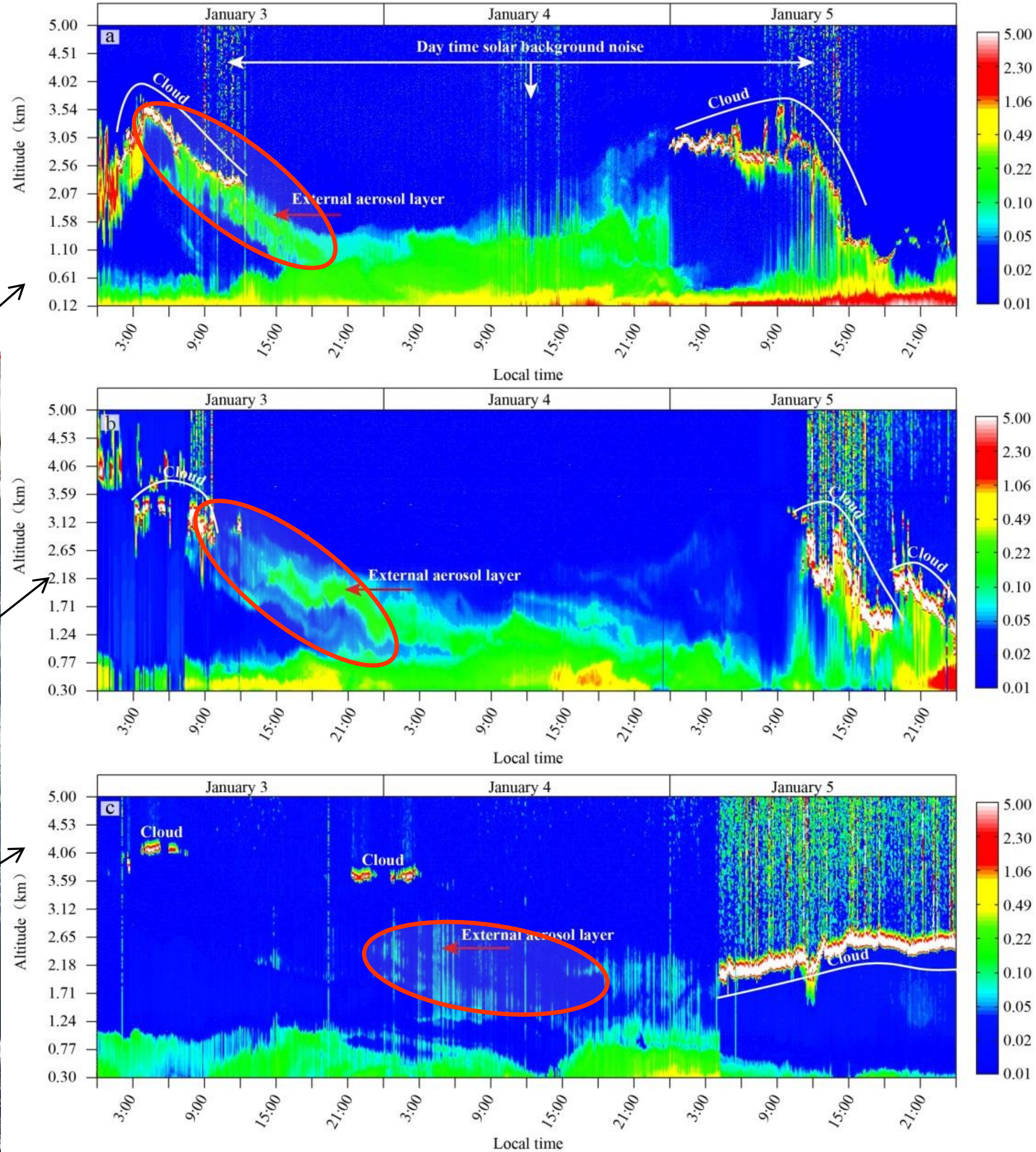

The high altitude wind fields (700 and 750 hPa) at 2:00am on 3 January show north-westerly prevailed in most polluted provinces, which favours the transport of pollutants from Hebei and Henan to Shandong and from Henan and Hubei by way of Anhui to Jiangsu.

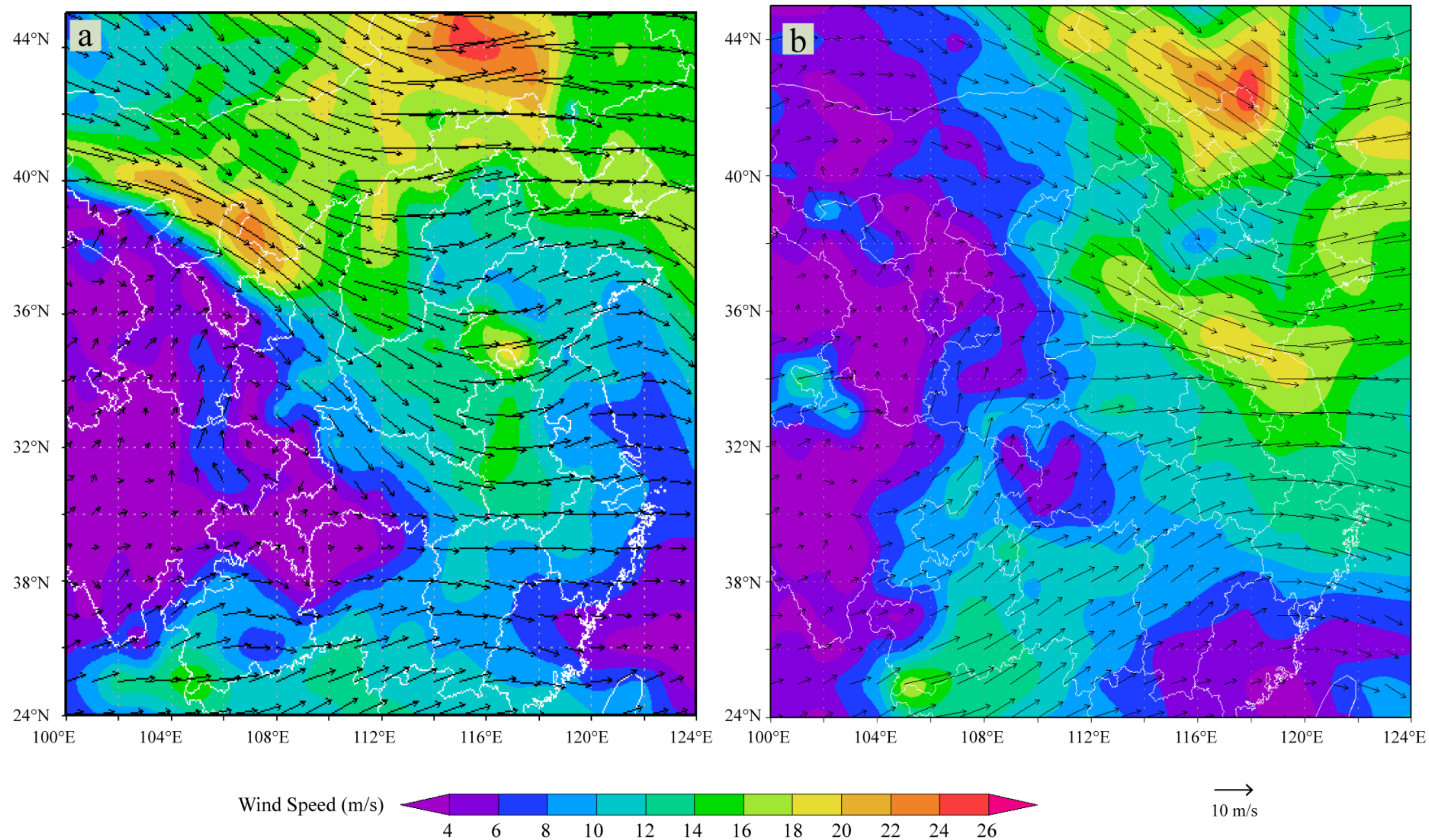

Part 3

Mapping surface NO_2 concentrations

Ground level NO_2 accounts for the majority of tropospheric NO_2 columns

Nanjing May, 2013 – Feb., 2015 provided by *Nan Hao* from EUMETSAT

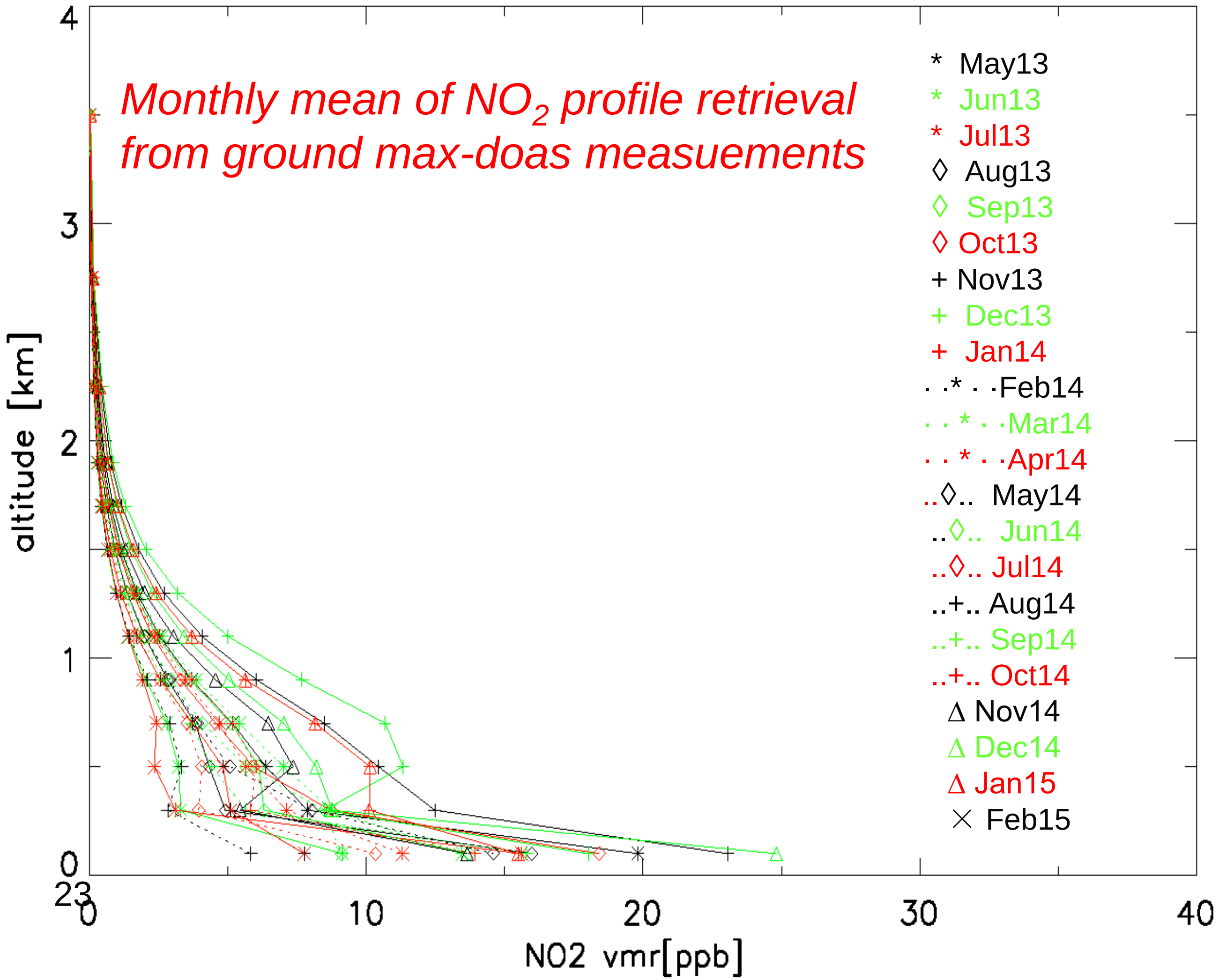

Most profiles peak at surface.

Three layers can be distinguished:

0-200 m, 200-400m and above 400 m.

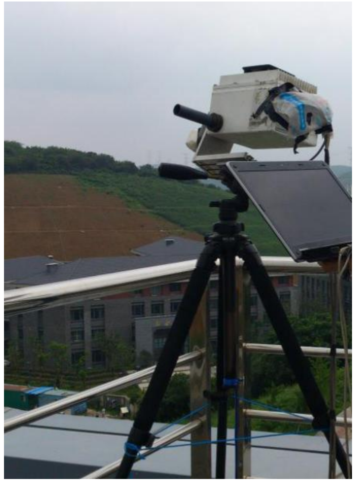

The Ozone Monitoring Instrument (OMI)

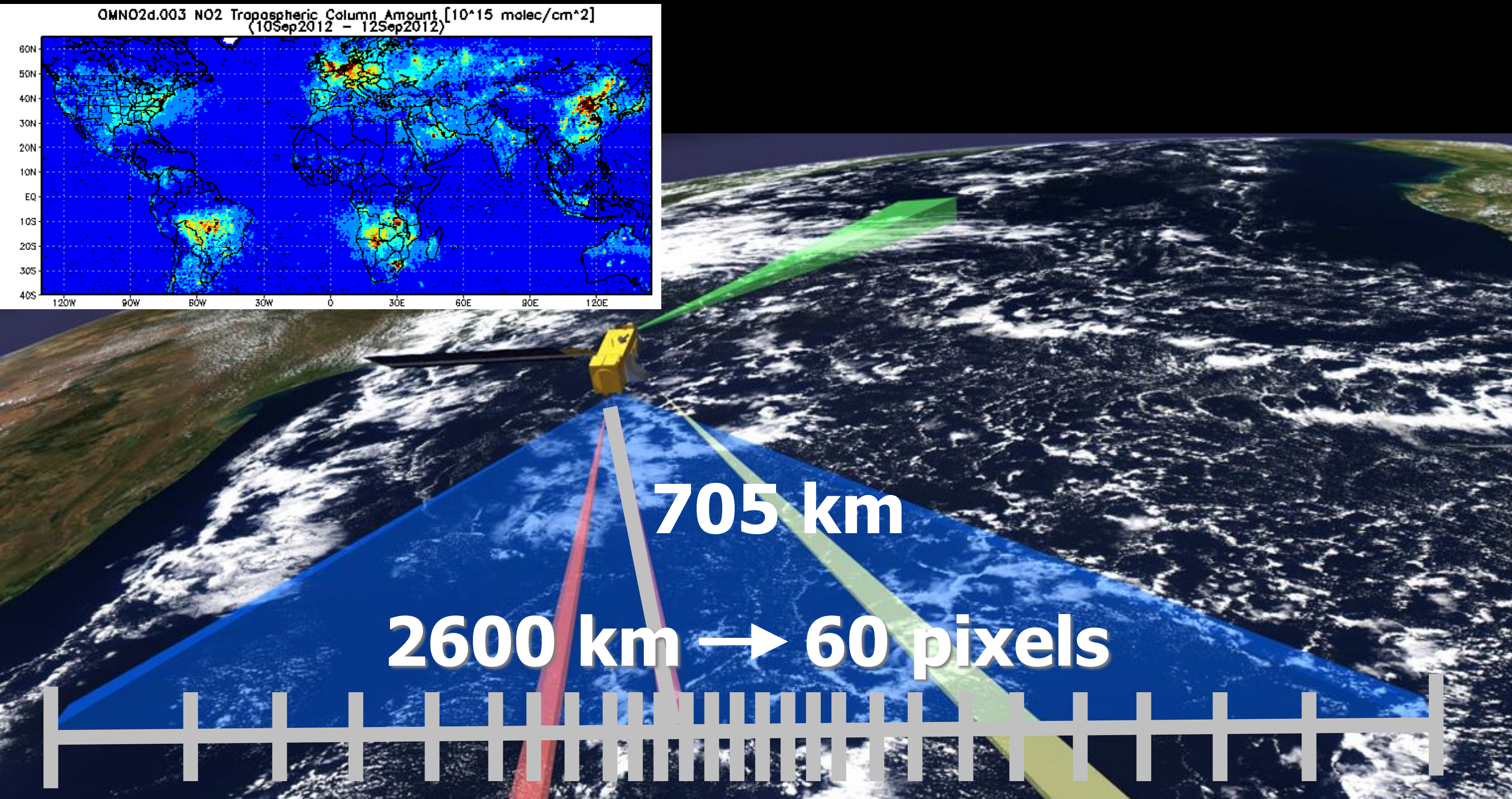

Detection limit = 5 × 10^{14} molec cm^{-2} ≈ 0.2 ppb

General Approach to Estimate Surface NO_2 Concentration

Daily OMI NO_2 Column

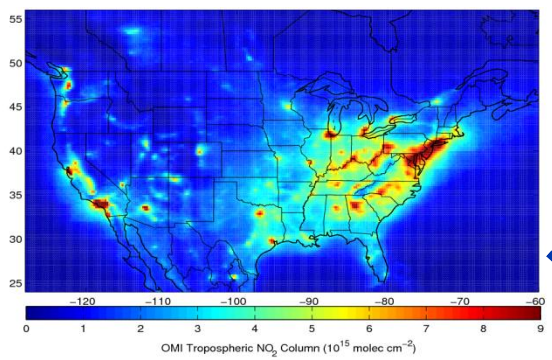

Lamsal et al. (2008, 2013)

Chemical Transport Model (CTM) Profile

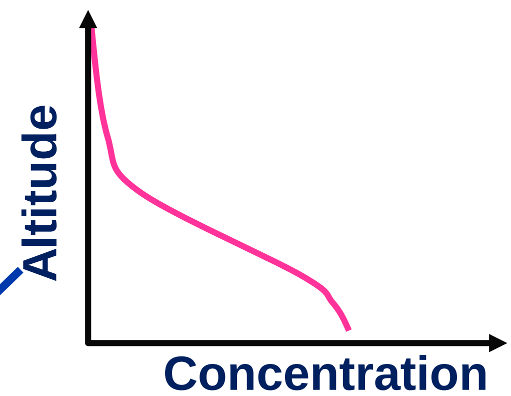

$$S_O = \Omega_O \left[\frac{S_M}{\Omega_M} \right]$$

S → Surface Concentration

Ω → Tropospheric column

- Emission inventories used for the model simulations are based on outdated statistical data, the profiles may not capture the actual vertical distribution
- **We introduce a geographically and temporally weighted regression (GTWR) model to estimate the ground level NO_2 concentrations using OMI tropospheric columns**

Geographically and Temporally Weighted Regression

- GTWR model was developed to deal with the spatial and temporal non-stationary issues *(Huang et al., 2010)*.
- The GTWR model for the relationship of ground NO_2 and satellite tropospheric columns can be expressed as:

$$NO_{2\_ground(i)} = \beta_0(u_i,v_i,t_i) + \beta_1(u_i,v_i,t_i) \times NO_{2\_Trop(i)} + \beta_2(u_i,v_i,t_i) \times RH_{(i)} + \beta_3(u_i,v_i,t_i) \times T_{(i)} + \beta_4(u_i,v_i,t_i) \times PBLH_{(i)} + \beta_5(u_i,v_i,t_i) \times WS_{(i)} + \beta_6(u_i,v_i,t_i) \times P_{(i)} + \varepsilon_i, (i = 1,2,\ldots,n)$$

NO_2 from ambient stations

Coordinates of the training sample i in location (u_i, v_i) at time t.

OMI NO_2 column density

$\beta_1(u_i,v_i,t_i)$, $\beta_2(u_i,v_i,t_i)$, $\beta_3(u_i,v_i,t_i)$, $\beta_4(u_i,v_i,t_i)$, $\beta_5(u_i,v_i,t_i)$, and $\beta_6(u_i,v_i,t_i)$ are the coefficients describing the unique spatial and temporal relationship between ground NO_2 and satellite tropospheric columns, denoting the slopes of *T*, *RH*, *PBLH*, *WS*, and *P*, respectively.

Akaike's information criterion (AIC) was used to judge whether the GTWR performance could be improved with the addition of each specific meteorological parameter.

Experiment Results

The relationship between tropospheric-columnar and ground-level NO_2

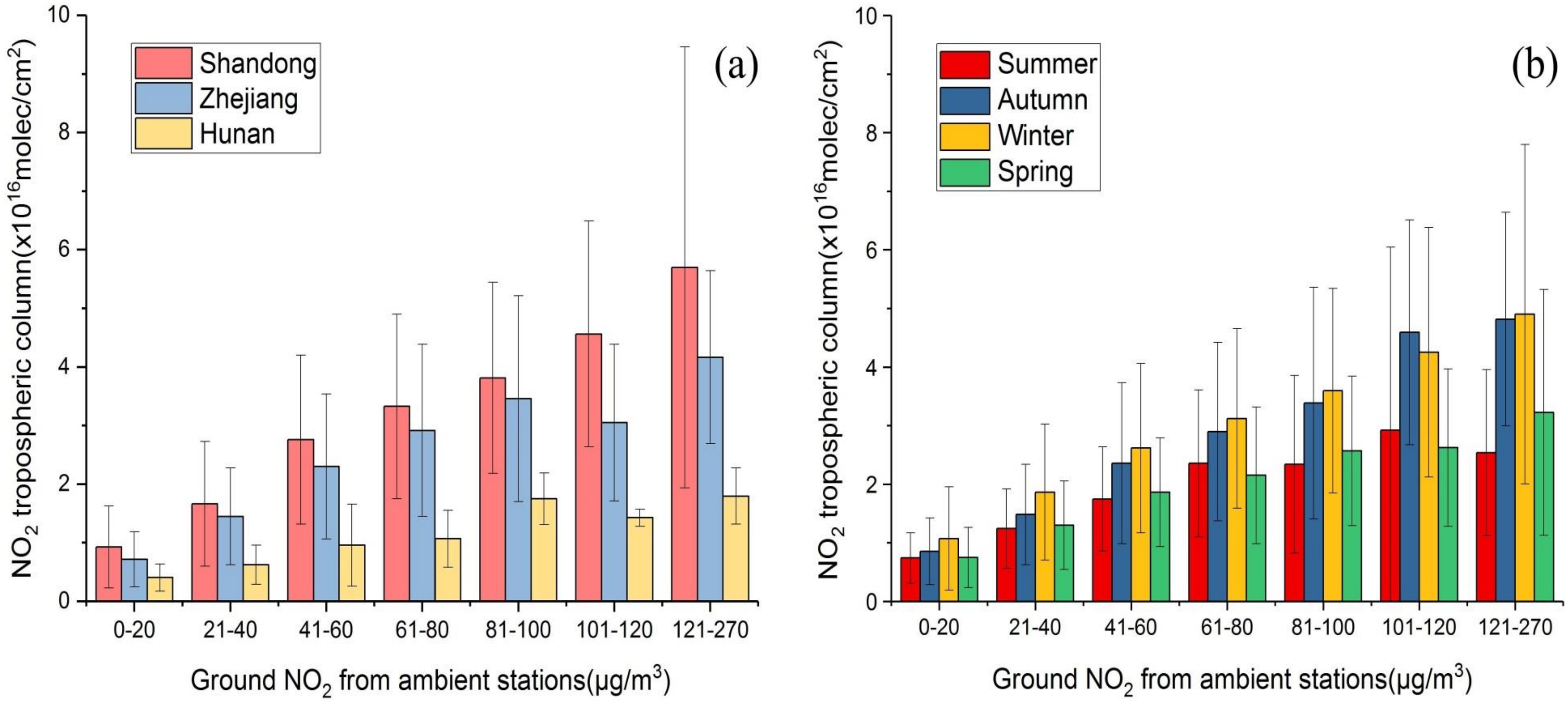

Significant geographical and seasonal variations!

Experiment Results

The comparison of GTWR method with chemistry transport model (CTM) method

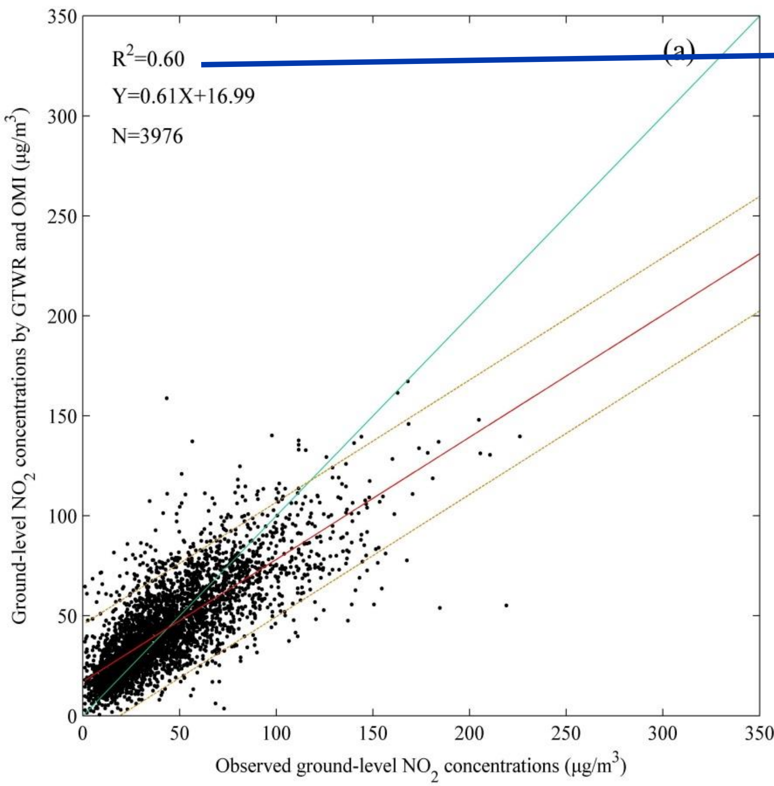

The coefficient of determination (R^2) of 0.60 obtained by the GTWR method is comparable to the correlation coefficient (R) of 0.80 achieved by *Gu et al* using the CTM method.

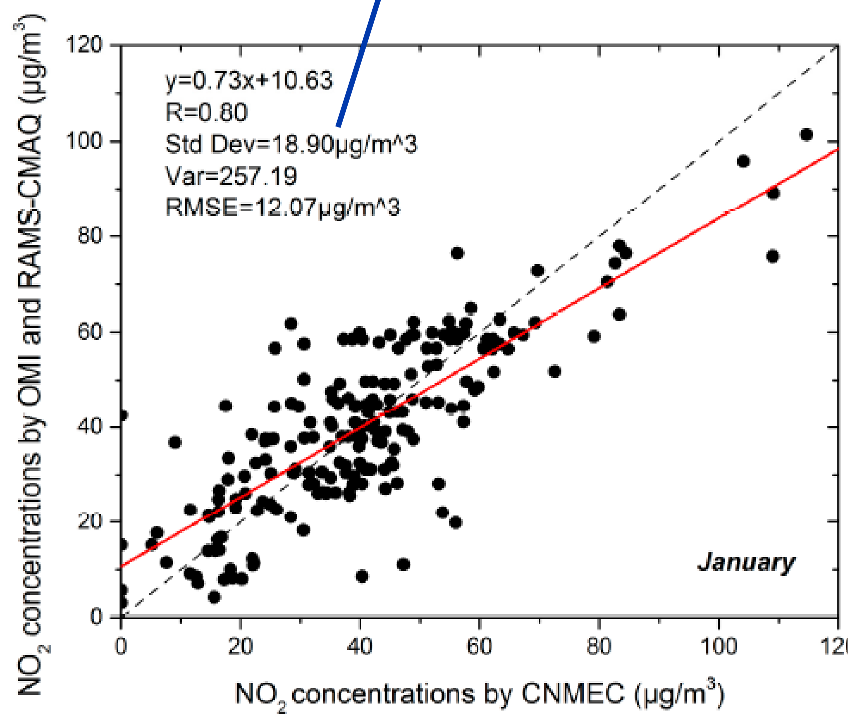

Experiment Results

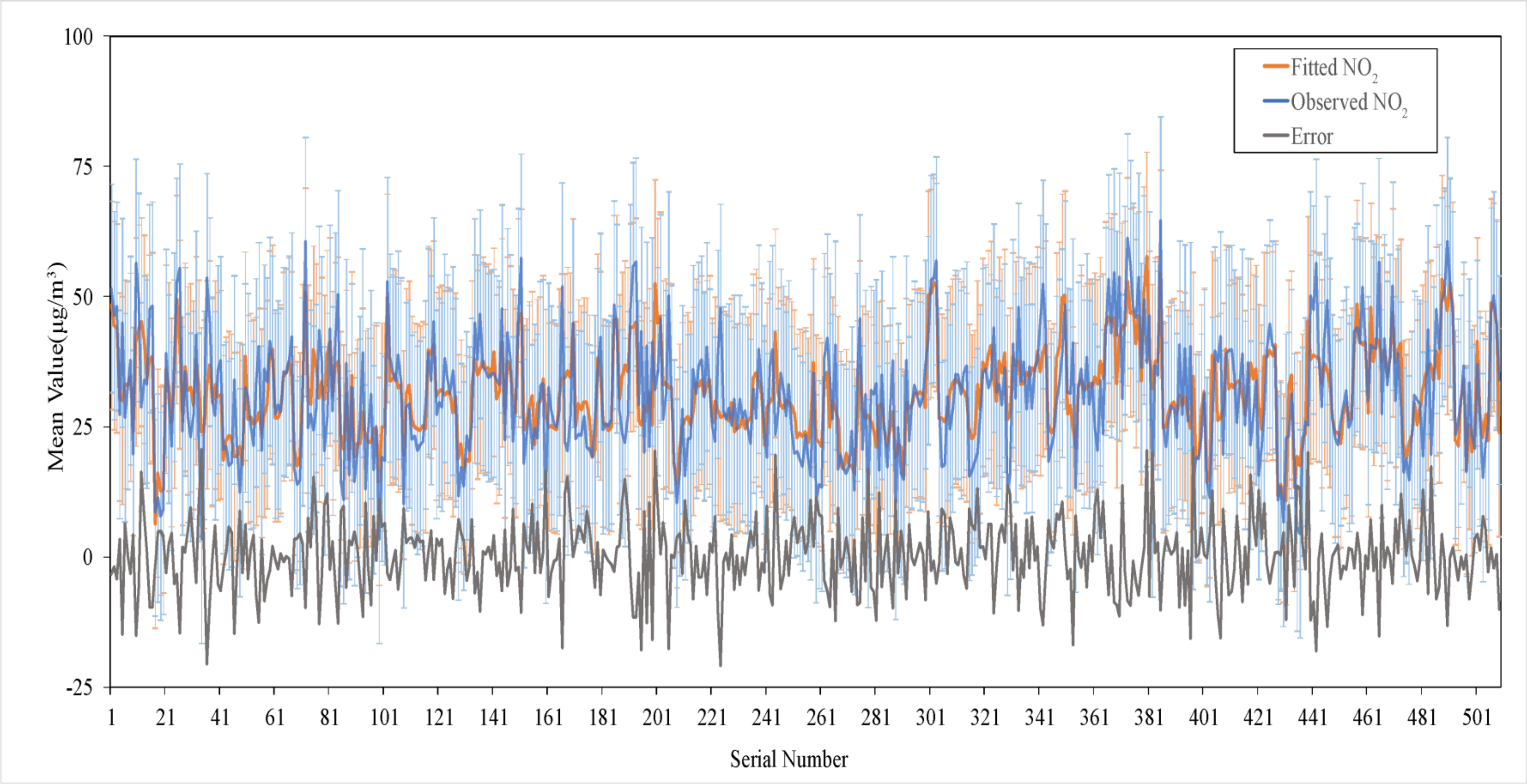

More than 90% of the cross-validation stations possess low mean discrepancies less than 10 μg/m^3.

Experiment Results

Spatial distributions of annually-mean NO_2 values

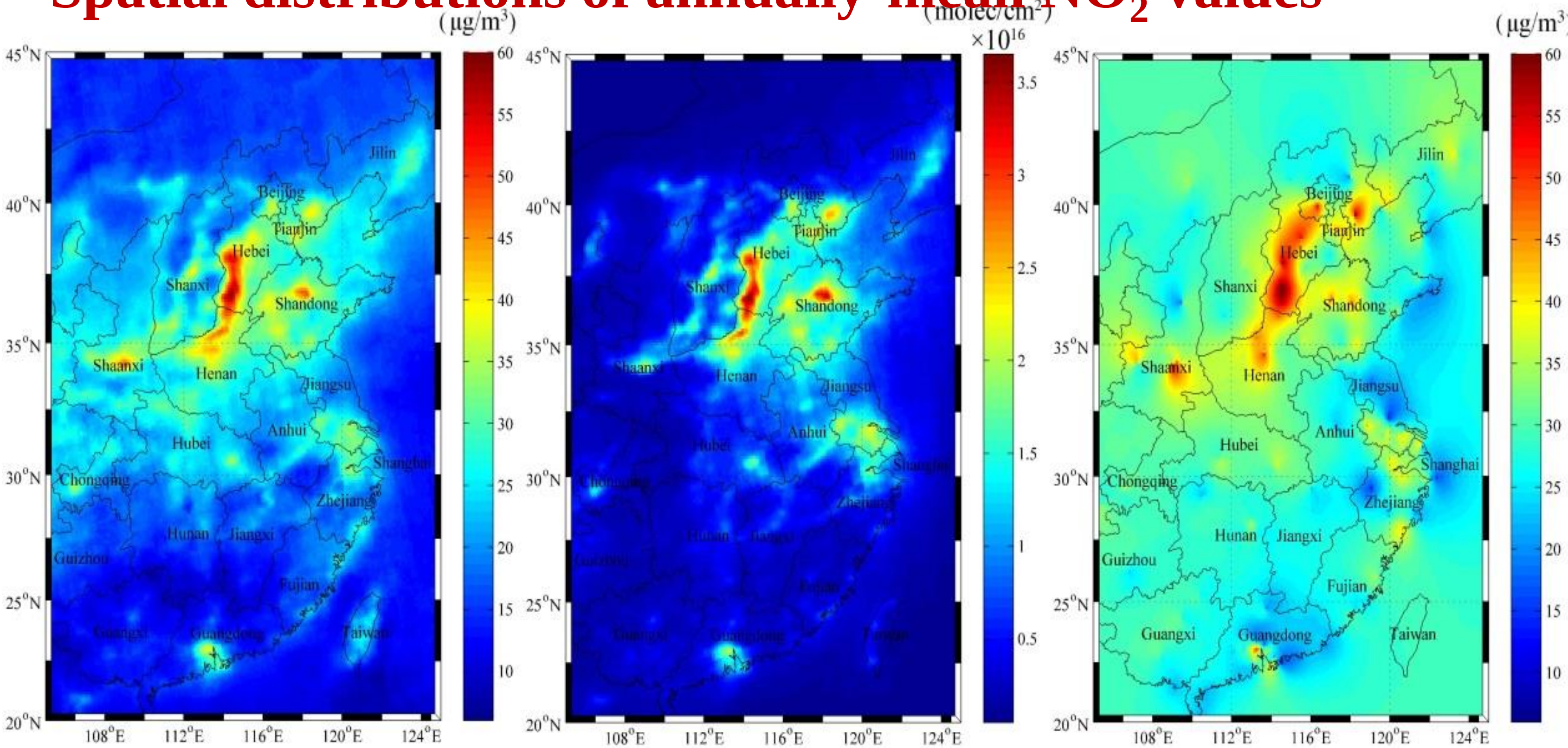

(a) GTWR fitted ground-level NO_2 (b) Tropospheric NO_2 columns (c) Interpolated ground-level NO_2

The GTWR fitted ground NO_2 in (a) has a similar spatial pattern to the satellite tropospheric NO_2 column in (b). The concentrations are comparable to the interpolated in situ observations using the Kriging method in (c) over the region with high values.

References

- Qin K，Wang L，Wu L X， et al. A campaign for investigating aerosol optical properties during winter hazes over Shijiazhuang, China. Atmospheric Research, 198: 113-122, 2017.
- Qin, K. Rao, L.; Xu, J.; Bai, Y.; Zou, J.; Hao, N.; Li, S.; Yu, C. Estimating Ground Level NO2 Concentrations over Central-Eastern China Using a Satellite-Based Geographically and Temporally Weighted Regression Model. Remote Sens. 2017, 9, 950.
- Wong M S，Qin K*，Lian H，et al. Continuous ground-based aerosol Lidar observation during seasonal pollution events at Wuxi，China. Atmospheric Environment，154: 189-199, 2017.
- 滕继峣，秦凯*，汪云甲，等.基于激光雷达观测的大气边界层自动识别局部最优点算法.光谱学与光谱分析，37(2): 361-367, 2017.
- Qin K，Wu L X，Wong M S，et al. Trans-boundary aerosol transport during a winter haze episode in China revealed by ground-based Lidar and CALIPSO satellite. Atmospheric Environment，141: 20-29，2016.
- Bai Y, Wu L, Qin K, et al. A geographically and temporally weighted regression model for ground-level PM2. 5 estimation from satellite-derived 500 m resolution AOD. Remote Sensing, 2016, 8(3): 262.
- 郎红梅，秦凯*，袁丽梅，等. 徐州冬季雾-霾天颗粒物粒径及气溶胶光学特性变化特征. 中国环境科学，36(8): 2260-2269，2016.
- 吴立新，吕鑫，秦凯，等. 基于太阳光度计地基观测的徐州气溶胶光学特性变化分析. 科学通报，20: 2287-2298，2016
- 胡明玉，秦凯*，白杨，等. 2013 年 12 月石家庄一次霾天气过程中的黑炭浓度特征. 中国环境科学，35(9): 2585-2593，2015
- 吴立新，吕鑫，秦凯，等. 秸秆焚烧期间徐州市空气污染物时空分布特征分析. 地理与地理信息科学，30(1): 18-22，2014.
- 白杨，秦凯，吴立新，等. 徐州市区主干道路黑炭气溶胶浓度移动观测实验. 地理与地理信息科学，30(1): 45-49，2014.